Quantum Thermal Machine as a Thermometer

Patrick P. Hofer,[1,*] Jonatan Bohr Brask,[1] Martí Perarnau-Llobet,[2,3] and Nicolas Brunner[1]
[1]Département de Physique Appliquée, Université de Genève, 1211 Genève, Switzerland
[2]Max-Planck-Institut für Quantenoptik, Hans-Kopfermann-Str. 1, D-85748 Garching, Germany
[3]ICFO-Institut de Ciencies Fotoniques, The Barcelona Institute of Science and Technology, 08860 Castelldefels, Barcelona, Spain
(Received 21 March 2017; revised manuscript received 29 May 2017; published 1 September 2017)

We propose the use of a quantum thermal machine for low-temperature thermometry. A hot thermal reservoir coupled to the machine allows for simultaneously cooling the sample while determining its temperature without knowing the model-dependent coupling constants. In its most simple form, the proposed scheme works for all thermal machines that perform at Otto efficiency and can reach Carnot efficiency. We consider a circuit QED implementation that allows for precise thermometry down to ∼15 mK with realistic parameters. Based on the quantum Fisher information, this is close to the optimal achievable performance. This implementation demonstrates that our proposal is particularly promising in systems where thermalization between different components of an experimental setup cannot be guaranteed.

DOI: 10.1103/PhysRevLett.119.090603

Introduction.—Accurate sensing and measuring of temperature is of crucial importance throughout natural science and technology. Increased capabilities of control and imaging on smaller and smaller scales have led to the need for precise thermometry down to millikelvin temperatures at submicron scales. Conventional techniques are not applicable in this regime, resulting in the development of a broad range of new methods over the last decade [1]. Many of these employ probes that are so small that quantum effects become relevant in their design and sensing capabilities, e.g., quantum dots [2–4], nitrogen-vacancy centers in diamond [5–7], superconducting quantum interference devices [8], and even biomolecules [9]. At the same time, the study of thermal processes in the quantum regime has recently seen increased interest fueled by tools developed in quantum information theory [10,11]. This approach has led to novel insights into the limitations of measuring cold temperatures posed by quantum theory [12–16], showing that coherence can be beneficial for low-temperature thermometry [12,17–20].

In a standard approach to thermometry, a probe is brought into thermal contact with the sample and the system is allowed to equilibrate [3,4]. The temperature is then read out through some observable on the probe whose relation to the temperature is known. The measurement can possibly be improved by letting the probe interact with the sample for a finite time only, making use of the transient dynamics [17,21], or by increasing the coupling strength between sample and probe [22]. Both of these approaches lead to a nonequilibrium state for the probe. Another approach to thermometry, which is employed to measure electronic temperatures, makes use of a voltage bias that creates an out-of-equilibrium situation. The temperature can then be determined through the current-voltage characteristics [23–25]. We note that these strategies generally lead to unwanted heating of the sample.

In this Letter, we connect thermometry to quantum thermal machines. Such machines are extensively studied to investigate fundamental as well as practical aspects of quantum thermodynamics [10,26–29]. By construction, these machines constitute out-of-equilibrium systems including a temperature gradient. Here we consider a quantum refrigerator to simultaneously cool the sample

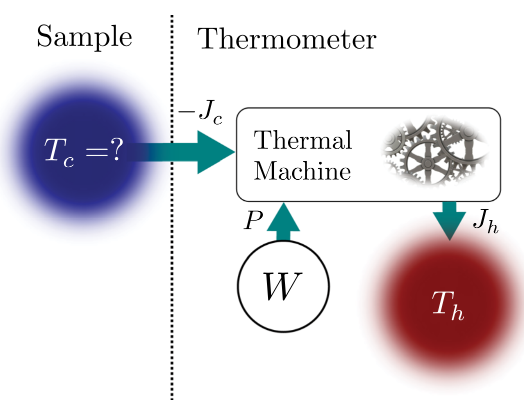

FIG. 1. Sketch of the thermometer. In order to measure the temperature of the cold bath, a quantum thermal machine is operated as a refrigerator, inducing a heat current from the cold bath to the hot bath. This requires energy from the work source W. The hot temperature is then increased until the machine reaches the Carnot point where its power consumption and the heat flows vanish (i.e., $P = J_c = J_h = 0$). For machines that perform with a well-known efficiency (e.g., the Otto efficiency $\eta = 1 - \Omega_c/\Omega_h$), the cold temperature can then be deduced from the hot temperature through the relation $\eta = \eta_C = 1 - T_c/T_h$, without the need of knowing any model-dependent coupling constants. In this way, a low precision measurement of a hot temperature is converted into a high precision measurement of a low temperature. Operating the thermal machine as a refrigerator avoids any heating of the cold bath.

and estimate its temperature. This way, the proposed thermometer does not induce any heating of the sample, even if it is at the coldest temperature that is experimentally available. Our proposal thus makes use of a thermal bias to create an out-of-equilibrium situation that is favorable for thermometry. This idea goes back to Thomson (Lord Kelvin), who considered the use of a Carnot engine to determine an absolute temperature scale [30] (see also Ref. [31]). Note that albeit the thermal bias, the sample is assumed to remain in local equilibrium throughout the measurement.

The main idea is illustrated in Fig. 1. The sample to be measured is a thermal bath at a cold temperature T_c. Through a small quantum system (the machine), the sample is coupled to another bath at a higher temperature T_h and an external power source (which, in principle, could be provided by a third thermal bath [32–35]). Note that this setup can operate either as a refrigerator, with the power source driving a heat flow from the cold to the hot bath, or as a heat engine, where work is generated using a heat flow from the hot to the cold bath [27,36–41]. Since we are interested in determining T_c, the whole setup, apart from the cold bath, should be considered as the thermometer. By operating the machine as a refrigerator, the sample will be cooled during the measurement of T_c, avoiding any undesirable heating. Furthermore, by approaching the Carnot point, where the machine approaches reversibility, the need for knowledge of the coupling constants can be eliminated, just as for thermalizing thermometry. We note that some knowledge of the hot bath temperature is required for our scheme. However, the cold temperature can be determined with high precision even if the hot temperature measurement is noisy. Our scheme can thus be seen as a method to turn an uncertain measurement of warm temperatures into precise measurements of cold temperatures working similarly to a Wheatstone bridge, where resistors of known resistances are used to determine an unknown resistance.

The rest of this Letter is structured as follows. After describing the working principle of the proposed thermometer in more detail, we discuss an implementation in a circuit QED architecture, which allows for precise thermometry of a microwave resonator down to ∼15 mK using realistic parameters. Finally, we investigate the precision of the thermometer using the quantum Fisher information (QFI).

Scheme.—We now turn to a more detailed description of our thermometer. The thermal bias and the power source induce energy flows denoted by J_α (heat flow into bath α) and P (power consumption; see Fig. 1). The power consumed by the machine is in general a function of the temperatures as well as the model-dependent parameters. Inverting this relationship, the cold temperature can be written as $T_c = f(P, T_h)$. Here, f might have a complicated dependence on the model-dependent parameters. However, the relation simplifies for machines that perform at the Otto efficiency and exhibit a Carnot point [42]. When the machine is operated as a heat engine, the efficiency is defined as $\eta = P/J_h$. The Otto efficiency is given by $\eta = 1 - \Omega_c/\Omega_h$ where Ω_c, Ω_h are frequencies that depend on the architecture of the machine (see Fig. 2). For thermal machines that exhibit a Carnot point, setting the frequencies such that the efficiency is equal to the Carnot efficiency, $\eta_C = 1 - T_c/T_h$, results in vanishing energy flows. Examples of thermal machines that operate at the Otto efficiency and exhibit a Carnot point are discussed in Refs. [28,43–48]. We note that whenever the frequencies and temperatures are such that $\eta > \eta_C$, the machine operates as a refrigerator. At the Carnot point, we find the simple relation

$$T_c = \frac{\Omega_c}{\Omega_h} T_h, \tag{1}$$

implying that $f(P = 0, T_h) = T_h \Omega_c/\Omega_h$ is independent of any coupling constants. The above relation is a key ingredient for the proposed thermometer [see Supplemental Material for a discussion on imperfections that prevent Eq. (1) [49]]. In order to reach the Carnot point, one can either modify the frequencies Ω_α or the temperature T_h associated with the thermometer. Here we focus on the case where the frequencies remain fixed but one has some control over $T_h > T_c$. The cold temperature can then be determined using the following strategy (see Fig. 3). (1) Initiate the machine to act as a refrigerator, i.e., $T_h < T_c \Omega_h/\Omega_c$, and monitor P. (2) Increase T_h until $P = 0$ is reached. (3) Measure T_h. (4) Determine T_c using Eq. (1).

In this scheme, two quantities are measured to determine T_c: The power consumption P and the hot temperature T_h. Both of these measurements are accompanied by errors, ΔP and ΔT_h. Simple error propagation yields (assuming independent errors)

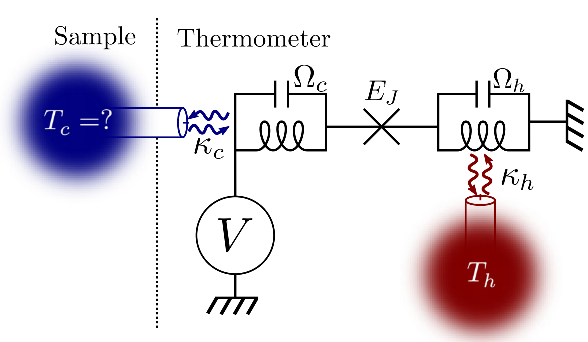

FIG. 2. Circuit QED implementation of the thermometer. Two harmonic oscillators with frequencies Ω_h and Ω_c are coupled to thermal baths at temperatures T_c and T_h, respectively, and to each other through a Josephson junction. The external bias voltage V ensures that the cold bath is being cooled while determining T_c.

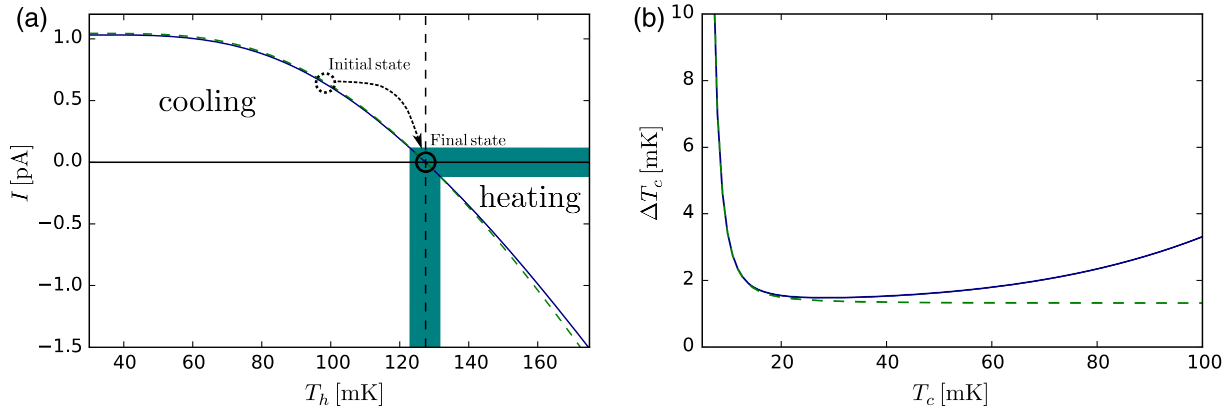

FIG. 3. Performance of a circuit QED implementation. (a) Charge current as a function of the hot temperature T_h for fixed $T_c = 15$ mK. The refrigerator is initiated at T_h below the Carnot point (dotted circle), leading to cooling of the cold bath. T_h is then increased until the current vanishes (solid circle). This point can only be determined up to a certain error ΔI that induces an uncertainty in the final T_h (shaded area). (b) Error in the temperature estimation, Eq. (2). Measurement errors of $\Delta I = 0.3$ pA and $\Delta T_h = 10$ mK lead to $\Delta T_c < 2$ mK down to temperatures of 15 mK. Blue (solid) lines are numeric solutions; green (dashed) lines are obtained analytically using a simplified model [49]. Parameters: $\Omega_h = 2\pi \times 8.5$ GHz, $\Omega_c = 2\pi \times 1$ GHz, $\kappa_h = \kappa_c = 2\pi \times 0.06$ GHz, $E_J = 2\pi \times 0.2$ GHz, $\lambda_h = \lambda_c = 0.3$.

$$\Delta T_c = \sqrt{\left(\frac{\partial f}{\partial P}\right)^2 (\Delta P)^2 + \left(\frac{\partial f}{\partial T_h}\right)^2 (\Delta T_h)^2}. \tag{2}$$

The error thus depends on the derivatives of f, which generally depend on model-specific parameters. Note however that $\partial_{T_h} f|_{P=0} = \Omega_c/\Omega_h$, implying that the error induced by the measurement of T_h only depends on the frequencies. Any uncertainty in the measurement of T_h can thus be compensated by increasing the ratio Ω_h/Ω_c and thus does not represent a fundamental limit.

Circuit QED implementation.—We now turn to an implementation of these ideas, considering the heat engine proposed in Ref. [47] and sketched in Fig. 2. In this machine, the quantum system consists of two LC oscillators with frequencies Ω_c and Ω_h coupled to each other through a Josephson junction. Such a system has recently been implemented experimentally, investigating the emission of nonclassical radiation [54]. See also Refs. [55–57] for related experiments. Each oscillator is coupled individually to a heat bath, one of which is the sample at temperature T_c, and the power source is provided by an external voltage bias V. We note that a similar setup (without any temperature bias however) has been considered for thermometry in Ref. [58]. The Hamiltonian describing the system reads (in a rotating frame)

$$\hat{H} = \frac{E_J}{2}(\hat{a}_h^\dagger \hat{A}_h \hat{A}_c \hat{a}_c + \text{H.c.}), \tag{3}$$

where E_J is the Josephson energy, $\hat{a}_\alpha$ annihilates a photon in the oscillator with frequency Ω_α, and the nonlinear operators $\hat{A}_\alpha$ are defined as

$$\hat{A}_\alpha = 2\lambda_\alpha e^{-2\lambda_\alpha^2} \sum_{n_\alpha=0}^{\infty} \frac{L_{n_\alpha}^{(1)}(4\lambda_\alpha^2)}{n_\alpha + 1} |n_\alpha\rangle\langle n_\alpha|, \tag{4}$$

with $L_n^{(k)}(x)$ denoting the generalized Laguerre polynomials and where we defined the Fock states $\hat{a}_\alpha^\dagger \hat{a}_\alpha |n_\alpha\rangle = n_\alpha |n_\alpha\rangle$. We note that Eq. (3) is derived using a rotating wave approximation that holds under the resonance condition $2eV = \Omega_h - \Omega_c$ (for details, see Ref. [47]).

The evolution of the system in contact with the thermal baths is captured by a local Lindblad master equation

$$\begin{aligned}\partial_t \hat{\rho} = &-i[\hat{H}, \hat{\rho}] + \kappa_h (n_B^h + 1)\mathcal{D}[\hat{a}_h]\hat{\rho} + \kappa_h n_B^h \mathcal{D}[\hat{a}_h^\dagger]\hat{\rho} \\ &+ \kappa_c (n_B^c + 1)\mathcal{D}[\hat{a}_c]\hat{\rho} + \kappa_h n_B^c \mathcal{D}[\hat{a}_c^\dagger]\hat{\rho},\end{aligned} \tag{5}$$

where we defined $\mathcal{D}[\hat{A}]\hat{\rho} = \hat{A}\hat{\rho}\hat{A}^\dagger - \{\hat{A}^\dagger \hat{A}, \hat{\rho}\}/2$, κ_α denotes the energy damping rate associated with the bath α, and $n_B^\alpha = [\exp(\Omega_\alpha/k_B T_\alpha) - 1]^{-1}$ is the corresponding occupation number. In accordance with existing theory [59] and experiment [57], we neglect voltage fluctuations arising from a low-frequency environment. We note that the local master equation, Eq. (5), was recently shown to capture the thermodynamics of the considered heat engine very well [60,61]. Alternatively one may also consider a master equation based on a Floquet formalism; see Refs. [62–64].

The power consumption of the machine is $P = IV$, where $I = \langle \hat{I} \rangle$ is the (dc) electrical current with the current operator

$$\hat{I} = -\frac{I_c}{2i}(\hat{a}_c^\dagger \hat{A}_c \hat{A}_h \hat{a}_h - \text{H.c.}), \tag{6}$$

and $I_c = 2eE_J$ is the critical current. The mean heat currents are defined as

$$J_\alpha = \Omega_\alpha \kappa_\alpha (\langle \hat{n}_\alpha \rangle - n_B^\alpha). \tag{7}$$

All averages are taken with respect to the steady-state solution of Eq. (5). For a more detailed discussion on the working principle of the heat engine and the involved approximations, we refer the reader to Ref. [47]. It can be shown that this machine does perform at the Otto efficiency and can reach the Carnot efficiency at vanishing power. Furthermore, a tunable hot temperature could be implemented by heating one of the LC oscillators using a microwave antenna. Therefore, this circuit QED engine exhibits all the features required to perform thermometry as discussed above.

Figure 3(a) shows the electrical current as a function of the hot temperature and sketches the scheme for measuring T_c. The error of the measurement is plotted in Fig. 3(b). We find a precision of $\Delta T_c \lesssim 2$ mK for temperatures down to $T_c \sim 15$ mK. In accordance with Ref. [47], we find good quantitative agreement with an approximate model obtained from Eq. (3) by replacing the nonlinear operators $\hat{A}_\alpha$ by constants times the identity [49]. This model can be solved analytically and is used below to estimate the performance of our scheme using the quantum Fisher information. We note that instead of the electrical current, one could also measure the heat currents to determine the Carnot point.

Throughout this paper, we consider the thermometer as a device to determine the temperature of the cold bath. However, in this particular implementation, the thermometer measures the temperature of the microwave mode with frequency Ω_c (see Supplemental Material for a discussion where this temperature is not equal to the bath temperature [49]). In situations where thermalization between different components of an experimental setup is difficult to achieve, our proposal thus provides a promising route to determine the physically relevant temperature. Furthermore, the precision obtained in our proposal compares well with electronic out-of-equilibrium thermometry [24].

Quantum Fisher information.—As already mentioned, the measurement error resulting from the hot temperature measurement is not of a fundamental nature since we can, in principle, reduce it by increasing Ω_h/Ω_c. In order to understand how well the current measurement is doing in terms of temperature estimation, we turn to the quantum Fisher information.

The steady-state solution of Eq. (5) defines a family of states as a function of T_c. The QFI with respect to T_c is a measure of the sensitivity of the state to changes in this parameter [65]. Through the quantum Cramer-Rao bound, it provides a lower bound on the mean-squared error in estimating T_c from any possible measurement [66]. Specifically,

$$(\Delta T_c)^2 \geq \frac{1}{\nu F_{T_c}} \equiv \frac{1}{\nu} (\Delta T_c)^2_{\mathrm{QFI}}, \tag{8}$$

where F_{T_c} is the QFI with respect to T_c and ν is the number of independent repetitions of the experiment. The bound is relevant (and can be saturated) in the local estimation regime, where the prior on the estimated parameter is narrow and many repetitions are performed. In the same regime, for measuring a specific observable $\hat{O}$, the attainable precision is given by the error propagation formula $(\Delta T_c)^2_{\hat{O}} \equiv (\Delta \hat{O})^2_\rho / |\partial_{T_c} \langle \hat{O} \rangle_\rho|^2$. Hence, by substituting the current operator for $\hat{O}$ and comparing $(\Delta T_c)_{\mathrm{QFI}}$ and $(\Delta T_c)_{\hat{I}}$ evaluated in the steady state at the Carnot point, we can get an idea of how close the current measurement is to being optimal. Note that this neglects any errors in other parameters as well as the fact that our strategy is based on continuous measurements rather than projective measurements. Although we should thus not expect this calculation to give us the actual uncertainty obtained in an experiment, it does tell us whether the current is a good choice of observable for estimating T_c.

To perform the comparison, we first need to find the steady-state solution of Eq. (5). This can be done analytically for the approximate model discussed in Supplemental Material [49] yielding $(\Delta T_c)_{\hat{I}_T} = \alpha T_c^2 \sinh(\Omega_c/2T_c)/\Omega_c$, and $(\Delta T_c)_{\mathrm{QFI}} = (\Delta T_c)_{\hat{I}_T} \beta/\alpha$, where the parameters α and β depend on the coupling constants and are given in Supplemental Material [49]. We see that the current-measurement precision and the optimal precision from the QFI have exactly the same functional behavior with temperature and energy, but depend differently on the coupling constants. For any choice of couplings, $\alpha \geq \beta$ such that $(\Delta T_c)_{\hat{I}_T} \geq (\Delta T_c)_{\mathrm{QFI}}$. Both expressions are plotted in Fig. 4. The reason that the current operator is a good observable for determining T_c is ultimately due to the fact that the current is very sensitive to the occupation number in the oscillators. Although the occupation numbers depend only very weakly on temperature at sufficiently low temperatures, measuring occupation numbers is in many scenarios still the optimal choice [67].

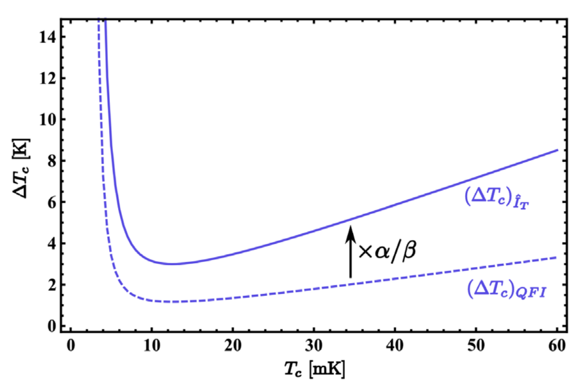

FIG. 4. Single-shot precision from a current measurement (blue solid) and from the QFI (blue dashed) at the Carnot point, for the simple model with oscillator frequencies and couplings given in the caption of Fig. 3, and fitting parameter $g = E_J/8$.

The smallest possible value of α is $4\sqrt{2}$, attained for $\kappa_c = \kappa_h = 2g$ (where g is the interaction strength in the approximate model). For the parameters used in Fig. 3, $\alpha/4\sqrt{2} \approx 1.02$, and so the current measurement is close to its best performance in this regime. Furthermore, $\alpha/\beta \approx 2.55$; hence, it is also not far from the optimal precision obtainable by any possible measurement. The smallest possible value of α/β is $\sqrt{2+\sqrt{2}} \approx 1.85$; however, it is attained in the weak coupling limit $\kappa_c \to 0$, where no information about T_c can be extracted and both α and β diverge.

Conclusion.—In conclusion, we investigated the use of thermal machines as thermometers. The nonequilibrium nature of the steady state in these systems allows for simultaneously cooling the cold bath while determining its temperature. Furthermore, our scheme only requires the measurement of the power consumption and the hot temperature, both of which do not require any projective measurements on the quantum system which are difficult to implement. For realistic parameters, an implementation in circuit QED allows for precise thermometry ($\Delta T_c \lesssim 2$ mK) of a microwave resonator mode down to small temperatures ($T_c \sim 15$ mK). While lower values have been reported (see, e.g., Ref. [24] where precise thermometry down to 6 mK has been reported) our scheme is of particular interest when thermalization between different components of an experimental setup cannot be guaranteed and heating of the sample has to be avoided. Our proposal can be readily adapted to other architectures.

We acknowledge interesting discussions with L. Correa. P. H., J. B., and N. B. acknowledge the Swiss National Science Foundation (starting Grant DIAQ, Grant No. 200021_169002, and QSIT). M. P.-L. acknowledges the Alexander von Humboldt Foundation, the CELLEX-ICFO-MPQ research fellowships, the Spanish MINECO (Grants No. QIBEQI FIS2016-80773-P and No. SEV-2015-0522), and the Generalitat de Catalunya (Grants No. SGR875 and CERCA Programme).

*patrick.hofer@unige.ch

[1] *Thermometry at the Nanoscale*, edited by L. D. Carlos and F. Palacio (The Royal Society of Chemistry, Cambridge, 2016).

[2] G. W. Walker, V. C. Sundar, C. M. Rudzinski, A W. Wun, M. G. Bawendi, and D G. Nocera, Quantum-dot optical temperature probes, Appl. Phys. Lett. **83**, 3555 (2003).

[3] F. Seilmeier, M. Hauck, E. Schubert, G. J. Schinner, S. E. Beavan, and A. Högele, Optical Thermometry of an Electron Reservoir Coupled to a Single Quantum Dot in the Millikelvin Range, Phys. Rev. Applied **2**, 024002 (2014).

[4] F. Haupt, A. Imamoglu, and M. Kroner, Single Quantum Dot as an Optical Thermometer for Millikelvin Temperatures, Phys. Rev. Applied **2**, 024001 (2014).

[5] D. M. Toyli, C. F. de las Casas, D. J. Christle, V. V. Dobrovitski, and D. D. Awschalom, Fluorescence thermometry enhanced by the quantum coherence of single spins in diamond, Proc. Natl. Acad. Sci. U.S.A. **110**, 8417 (2013).

[6] G. Kucsko, P. C. Maurer, N. Y. Yao, M. Kubo, H. J. Noh, P. K. Lo, H. Park, and M. D. Lukin, Nanometre-scale thermometry in a living cell, Nature (London) **500**, 54 (2013).

[7] P. Neumann, I. Jakobi, F. Dolde, C. Burk, R. Reuter, G. Waldherr, J. Honert, T. Wolf, A. Brunner, J. H. Shim, D. Suter, H. Sumiya, J. Isoya, and J. Wrachtrup, High precision nanoscale temperature sensing using single defects in diamond, Nano Lett. **13**, 2738 (2013).

[8] D. Halbertal, J. Cuppens, M. Ben Shalom, L. Embon, N. Shadmi, Y. Anahory, H. R. Naren, J. Sarkar, A. Uri, Y. Ronen, Y. Myasoedov, L. S. Levitov, E. Joselevich, A. K. Geim, and E. Zeldov, Nanoscale thermal imaging of dissipation in quantum systems, Nature (London) **539**, 407 (2016).

[9] J. S. Donner, S. A. Thompson, M. P. Kreuzer, G. Baffou, and R. Quidant, Mapping intracellular temperature using green fluorescent protein, Nano Lett. **12**, 2107 (2012).

[10] J. Goold, M. Huber, A. Riera, L. del Rio, and P. Skrzypczyk, The role of quantum information in thermodynamics—a topical review, J. Phys. A **49**, 143001 (2016).

[11] S. Vinjanampathy and J. Anders, Quantum thermodynamics, Contemp. Phys. **57**, 545 (2016).

[12] T. M. Stace, Quantum limits of thermometry, Phys. Rev. A **82**, 011611 (2010).

[13] U. Marzolino and D. Braun, Precision measurements of temperature and chemical potential of quantum gases, Phys. Rev. A **88**, 063609 (2013).

[14] L. A. Correa, M. Mehboudi, G. Adesso, and A. Sanpera, Individual Quantum Probes for Optimal Thermometry, Phys. Rev. Lett. **114**, 220405 (2015).

[15] M. G. A. Paris, Achieving the Landau bound to precision of quantum thermometry in systems with vanishing gap, J. Phys. A **49**, 03LT02 (2016).

[16] A. De Pasquale, D. Rossini, R. Fazio, and V. Giovannetti, Local quantum thermal susceptibility, Nat. Commun. **7**, 12782 (2016).

[17] S. Jevtic, D. Newman, T. Rudolph, and T. M. Stace, Single-qubit thermometry, Phys. Rev. A **91**, 012331 (2015).

[18] T. H. Johnson, F. Cosco, M. T. Mitchison, D. Jaksch, and S. R. Clark, Thermometry of ultracold atoms via nonequilibrium work distributions, Phys. Rev. A **93**, 053619 (2016).

[19] E. Martín-Martínez, A. Dragan, R. B. Mann, and I. Fuentes, Berry phase quantum thermometer, New J. Phys. **15**, 053036 (2013).

[20] C. Sabín, A. White, L. Hackermuller, and I. Fuentes, Impurities as a quantum thermometer for a Bose-Einstein condensate, Sci. Rep. **4**, 6436 (2014).

[21] L.-S. Guo, B.-M. Xu, J. Zou, and B. Shao, Improved thermometry of low-temperature quantum systems by a ring-structure probe, Phys. Rev. A **92**, 052112 (2015).

[22] L. A. Correa, M. Perarnau-Llobet, K. V. Hovhannisyan, S. Hernndez-Santana, M. Mehboudi, and A. Sanpera, Low-temperature thermometry enhanced by strong coupling, arXiv:1611.10123.

[23] F. Giazotto, T. T. Heikkilä, A. Luukanen, A. M. Savin, and J. P. Pekola, Opportunities for mesoscopics in thermometry and refrigeration: Physics and applications, Rev. Mod. Phys. **78**, 217 (2006).

[24] Z. Iftikhar, A. Anthore, S. Jezouin, F. D. Parmentier, Y. Jin, A. Cavanna, A. Ouerghi, U. Gennser, and F. Pierre, Primary thermometry triad at 6 mK in mesoscopic circuits, Nat. Commun. **7**, 12908 (2016).

[25] M. Zgirski, M. Foltyn, A. Savinnd, M. Meschkeand, and J. Pekola, Nanosecond thermometry with Josephson junction, arXiv:1704.04762.

[26] G. Benenti, G. Casati, K. Saito, and R. S. Whitney, Fundamental aspects of steady-state conversion of heat to work at the nanoscale, Phys. Rep. **694**, 1 (2017).

[27] R. Kosloff and A. Levy, Quantum heat engines and refrigerators: Continuous devices, Annu. Rev. Phys. Chem. **65**, 365 (2014).

[28] H. T. Quan, Yu-xi Liu, C. P. Sun, and F. Nori, Quantum thermodynamic cycles and quantum heat engines, Phys. Rev. E **76**, 031105 (2007).

[29] N. Brunner, N. Linden, S. Popescu, and P. Skrzypczyk, Virtual qubits, virtual temperatures, and the foundations of thermodynamics, Phys. Rev. E **85**, 051117 (2012).

[30] W. Thomson, On an absolute thermometric scale founded on Carnot's theory of the motive power of heat, and calculated from Regnault's observations, Proc. Cambridge Philos. Soc. **1**, 66 (1848).

[31] J. E. Geusic, E. O. Schulz-DuBois, and H. E. D. Scovil, Quantum equivalent of the Carnot cycle, Phys. Rev. **156**, 343 (1967).

[32] N. Linden, S. Popescu, and P. Skrzypczyk, How Small can Thermal Machines be? The Smallest Possible Refrigerator, Phys. Rev. Lett. **105**, 130401 (2010).

[33] P. Skrzypczyk, N. Brunner, N. Linden, and S. Popescu, The smallest refrigerators can reach maximal efficiency, J. Phys. A **44**, 492002 (2011).

[34] P. P. Hofer, M. Perarnau-Llobet, J. B. Brask, R. Silva, M. Huber, and N. Brunner, Autonomous quantum refrigerator in a circuit QED architecture based on a Josephson junction, Phys. Rev. B **94**, 235420 (2016).

[35] M. T. Mitchison, M. Huber, J. Prior, M. P. Woods, and M. B. Plenio, Realizing a quantum absorption refrigerator with an atom-cavity system, Quantum Sci. Technol. **1**, 015001 (2016).

[36] A. Levy and R. Kosloff, Quantum Absorption Refrigerator, Phys. Rev. Lett. **108**, 070604 (2012).

[37] M. T. Mitchison, M. P. Woods, J. P., and M. Huber, Coherence-assisted single-shot cooling by quantum absorption refrigerators, New J. Phys. **17**, 115013 (2015).

[38] R. Silva, P. Skrzypczyk, and N. Brunner, Small quantum absorption refrigerator with reversed couplings, Phys. Rev. E **92**, 012136 (2015).

[39] N. Brunner, M. Huber, N. Linden, S. Popescu, R. Silva, and P. Skrzypczyk, Entanglement enhances cooling in microscopic quantum refrigerators, Phys. Rev. E **89**, 032115 (2014).

[40] J. B. Brask and N. Brunner, Small quantum absorption refrigerator in the transient regime: Time scales, enhanced cooling, and entanglement, Phys. Rev. E **92**, 062101 (2015).

[41] A. Roulet, S. Nimmrichter, J. M. Arrazola, S. Seah, and V. Scarani, Autonomous rotor heat engine, Phys. Rev. E **95**, 062131 (2017).

[42] *Quantum Thermodynamics: Emergence of Thermodynamic Behavior within Composite Quantum Systems*, Lecture Notes in Physics Vol. 784 (Springer, Berlin, 2009).

[43] R. Kosloff, A quantum mechanical open system as a model of a heat engine, J. Chem. Phys. **80**, 1625 (1984).

[44] T. Feldmann and R. Kosloff, Quantum four-stroke heat engine: Thermodynamic observables in a model with intrinsic friction, Phys. Rev. E **68**, 016101 (2003).

[45] A. O. Niskanen, Y. Nakamura, and J. P. Pekola, Information entropic superconducting microcooler, Phys. Rev. B **76**, 174523 (2007).

[46] M. J. Henrich, F. Rempp, and G. Mahler, Quantum thermodynamic Otto machines: A spin-system approach, Eur. Phys. J. Spec. Top. **151**, 157 (2007).

[47] P. P. Hofer, J.-R. Souquet, and A. A. Clerk, Quantum heat engine based on photon-assisted Cooper pair tunneling, Phys. Rev. B **93**, 041418(R) (2016).

[48] M. Campisi and R. Fazio, The power of a critical heat engine, Nat. Commun. **7**, 11895 (2016).

[49] See Supplemental Material http://link.aps.org/supplemental/10.1103/PhysRevLett.119.090603 for analytical results using a simplified model and a discussion on the influence of heat leaks and spurious modes, which includes Refs. [50–53].

[50] A. Monras, Phase space formalism for quantum estimation of Gaussian states, arXiv:1303.3682.

[51] Z. Jiang, Quantum Fisher information for states in exponential form, Phys. Rev. A **89**, 032128 (2014).

[52] D. Šafránek and I. Fuentes, Optimal probe states for the estimation of Gaussian unitary channels, Phys. Rev. A **94**, 062313 (2016).

[53] C. Sparaciari, S. Olivares, and M. G. A. Paris, Gaussian-state interferometry with passive and active elements, Phys. Rev. A **93**, 023810 (2016).

[54] M. Westig, B. Kubala, O. Parlavecchio, Y. Mukharsky, C. Altimiras, P Joyez, D. Vion, P. Roche, M. Hofheinz, D Esteve, M Trif, P. Simon, J. Ankerhold, and F. Portier, Emission of nonclassical radiation by inelastic cooper pair tunneling, arXiv:1703.05009.

[55] T. Holst, D. Esteve, C. Urbina, and M. H. Devoret, Effect of a Transmission Line Resonator on a Small Capacitance Tunnel Junction, Phys. Rev. Lett. **73**, 3455 (1994).

[56] J. Basset, H. Bouchiat, and R. Deblock, Emission and Absorption Quantum Noise Measurement with an On-Chip Resonant Circuit, Phys. Rev. Lett. **105**, 166801 (2010).

[57] M. Hofheinz, F. Portier, Q. Baudouin, P. Joyez, D. Vion, P. Bertet, P. Roche, and D. Esteve, Bright Side of the Coulomb Blockade, Phys. Rev. Lett. **106**, 217005 (2011).

[58] O.-P. Saira, M. Zgirski, K. L. Viisanen, D. S. Golubev, and J. P. Pekola, Dispersive Thermometry with a Josephson Junction Coupled to a Resonator, Phys. Rev. Applied **6**, 024005 (2016).

[59] V. Gramich, B. Kubala, S. Rohrer, and J. Ankerhold, From Coulomb Blockade to Nonlinear Quantum Dynamics in a Superconducting Circuit with a Resonator, Phys. Rev. Lett. **111**, 247002 (2013).

[60] P. P. Hofer, M. Perarnau-Llobet, L. D. M. Miranda, G. Haack, R. Silva, J. B. Brask, and N. Brunner, Markovian

master equations for quantum thermal machines: Local vs global approach, arXiv:1707.09211.

[61] J. O. González, L. A. Correa, G. Nocerino, J. P. Palao, D. Alonso, and G. Adesso, Testing the validity of the local and global GKLS master equations on an exactly solvable model, arXiv:1707.09228.

[62] R. Alicki, D. A. Lidar, and P. Zanardi, Internal consistency of fault-tolerant quantum error correction in light of rigorous derivations of the quantum Markovian limit, Phys. Rev. A **73**, 052311 (2006).

[63] A. Levy, R. Alicki, and R. Kosloff, Quantum refrigerators and the third law of thermodynamics, Phys. Rev. E **85**, 061126 (2012).

[64] K. Szczygielski, D. Gelbwaser-Klimovsky, and R. Alicki, Markovian master equation and thermodynamics of a two-level system in a strong laser field, Phys. Rev. E **87**, 012120 (2013).

[65] A. S. Holevo, *Probabilistic and Statistical Aspect of Quantum Theory* (North-Holland, Amsterdam, 1982).

[66] S. L. Braunstein and C. M. Caves, Statistical Distance and the Geometry of Quantum States, Phys. Rev. Lett. **72**, 3439 (1994).

[67] S. Campbell, M. Mehboudi, G. De Chiara, and M. Paternostro, Global and local thermometry schemes in coupled quantum systems, arXiv:1705.01898.